On Energy-Relaxation for Transient Convection in Ferrofluids

Jitender Singh[1]

Abstract

The onset of transient instability driven by a coupling of thermal and magnetic effects in an initially quiescent ferrofluid layer is investigated using the energy method. Following the work of Kim et al. [Physics Letters, **A**, **372**, pp 4709-4713, (2008)], a new energy stability criterion is derived for the underlying dynamical system by taking into account the different boundary conditions and the Prandtl number effects. The critical onset time of the instability is determined as a function of the Rayleigh number, the Prandtl number, and the thermomagnetic parameter. For larger times, our analysis predicts that the energy stability theory and the linear theory yield essentially the same results irrespective of whether the fluid under consideration is a magnetically polarizable or a non-magnetic fluid and sub critical instabilities are not possible. For the global nonlinear stability boundary in the impulsively heated ferrofluid layer, the minimum critical onset time is found to occur when the values of the Rayleigh number and the thermomagnetic parameter are same.

AMS Classification: 76-XX, 76D17, 76E07

Keywords: Rayleigh-Bénard convection, Rapid heating, Ferromagnetic convection, Instability, Energy Stability, Rayleigh number

1 Introduction

The thermal convection in an initially quiescent, horizontal fluid-layer heated from below, is a typical model of natural convection occurring in atmosphere, oceans, and interior of stars and planets *etc.* The onset of instability in the layer is more popularly known as the Rayleigh-Bénard convection. The instability is known to manifest itself as a partitioning of the fluid layer into a steady polygonal pattern of convection cells. The fluid motion is identical within the convection cells. These results are well established theoretically and confirmed experimentally. For a quick introduction, interested reader may refer to the work of Chandrasekhar [1], Koschmieder [2], Drazin and Reid [3], Bodenschatz et al. [4] and references therein.

If the fluid layer is impulsively heated from below and cooled from the above, the basic state is a smooth function of time and it significantly affects the onset of instability. In such a transient system, the critical condition for the onset of the Rayleigh-Bénard convection is determined by

[1]Department of Mathematics, Guru Nanak Dev University, Amritsar-143005
E-mail: sonumaths@mail.com

the minimum time before which the basic transient state prevails. Thus, the critical stability boundary becomes time dependent.

To investigate the critical onset of instability in a hydrodynamical system, mainly two theories are employed: (i) linear theory which predicts the critical boundary above which the instability with respect to infinitesimal disturbances in the system is guaranteed [1, 3] and (ii) the nonlinear energy stability theory (Energy-Method), which predicts a critical boundary below which the stability of the system is guaranteed against arbitrary disturbances. A concise account of the energy stability theory and its results for the standard Rayleigh-Bénard convection in an initially quiescent fluid layer heated from below under different flow media, is given in Straughan [5].

Using energy method, Homsy [6] investigated the transient Rayleigh-Bénard convection and obtained the strong stability estimates for the permissible growth-rates of the disturbances. However his analysis was limited because of intense computational effort required to mark the marginal stability boundary.

Recently, Kim et al. [7] have extended the conventional energy method and proposed the relative energy stability concept. One merit of this approach is that it incorporates the effect of Prandtl number on the onset of instability which remained redundant in the previously existing conventional energy method.

An interesting feature of the Rayleigh-Bénard convection is this that at the onset of instability, the control parameter varies as the fourth-power of the wave number of disturbance when the wave number is significantly high. However for the onset of instability in a magnetized ferrofluid layer heated from above, the control parameter varies as the sixth power of the wave number (see Russel et al. [8, 9]). Such a fluid is controlled by a combined effect of the application of magnetic field and the temperature gradient [10, 11, 12]. This way applied magnetic field can also act as to control the ferromagnetic-convection which is an important aspect owing to the technological applications of ferrofluids.

A linear instability analysis of the Bénard convection in ferromagnetic fluids exposed to a vertical constant magnetic field, was first considered by Finlayson [13] who theoretically predicted a tight coupling between the buoyancy and the magnetic forces for the onset of instability.

Blennerhassett et al. [14] investigated linear and weakly nonlinear thermomagnetic instabilities in a strongly magnetized horizontal ferrofluid layer between rigid-planes, subjected to a strong-vertical uniform magnetic field and inferred a 10% rise in the Nusselt number when the lower boundary is hotter from its value in the absence of magnetic field.

It is well known that in the presence of applied magnetic field, the critical Rayleigh numbers for the energy stability boundary and the linear instability boundary coincide. The energy stability of the onset of steady ferrofluid convection has been carried out by Straughan [5]. However the onset of transient convection in ferrofluids subjected to impulsive heating, has not been investigated yet. Therefore, it is important to investigate the energy stability of such a problem and the objective of present study is to obtain the global nonlinear critical stability boundary for the onset of the transient ferrofluid convection by employing the relative-stability concept.

Rest of the paper is organized as follows. The problem is described in the Sec. 2 and the appropriate stability equations are obtained in this section. The nonlinear energy stability of the basic state is discussed in the Sec. 3. The numerical methods used for solving the underlying system of ODE's are described in Sec. 4. The numerical results so obtained are discussed in the same section. The possible conclusions from the results are made in the Sec. 5.

2 Mathematical Formulation

Consider a viscous, boussinesq ferrofluid layer of thickness d units, initially resting between two horizontal parallel upper and lower planes $z = d$, and $z = 0$, held at different temperatures T_2 and T_1 respectively, where $T_2,\ T_1 \in \mathbb{R},\ T_1 \neq T_2$, and $t \geq 0$ denotes the time variable. A constant vertical magnetic field $\mathbf{H}_0^{ext} = (0, 0, H_0^{ext})$ is applied to the ferrofluid layer. The system is governed by the following equations,

$$\rho_0 \frac{\partial \mathbf{u}}{\partial t} + \rho_0 \mathbf{u} \cdot \nabla \mathbf{u} = -\nabla p + \eta \nabla^2 \mathbf{u} + \rho \mathbf{g} + \mu_0 \mathbf{m} \cdot \nabla \mathbf{h}, \tag{2.1}$$

$$\nabla \cdot \mathbf{u} = 0, \tag{2.2}$$

$$\frac{\partial T}{\partial t} + \mathbf{u} \cdot \nabla T = k_T \nabla^2 T - \mu_0 T \frac{\partial \mathbf{m}}{\partial T} \cdot \left(\frac{\partial \mathbf{h}}{\partial t} + \mathbf{u} \cdot \nabla \mathbf{h} \right), \tag{2.3}$$

$$\nabla \cdot (\mathbf{m} + \mathbf{h}) = 0, \tag{2.4}$$

$$\nabla \times \mathbf{h} = \mathbf{0}, \tag{2.5}$$

where $\mathbf{u},\ p,\ T,\ \mathbf{h}$, and $\mathbf{m}$ are the fluid velocity, the fluid pressure, the fluid temperature, the magnetic field inside the fluid, and the fluid magnetization, respectively, at any time t; $\mathbf{g} = (0, 0, -g)$ is the acceleration due to gravity; ρ_0 is the fluid density at a reference temperature T_a; ρ and η are the density and the dynamic viscosity of the fluid, respectively, at a temperature T; μ_0 is the permeability constant; k_T is the thermal diffusivity. The fluid density ρ is a function of T in general and is given by the linear relation

$$\rho = \rho_0 \{1 - \alpha(T - T_a)\}, \tag{2.6}$$

where α is the coefficient of volume expansion. The magnetization $\mathbf{m}$ and the magnetic field $\mathbf{h}$ within the ferrofluid layer are related by

$$\mathbf{m} = \{m_0 + \chi(h - h_0) - K(T - T_a)\} \frac{\mathbf{h}}{h}, \tag{2.7}$$

where $\mathbf{m}_0$ is the fluid magnetization at a uniform magnetic field $\mathbf{h}_0$ of the ferrofluid layer when it is placed in an external magnetic field $\mathbf{H}_0^{ext}$ such that $H_0^{ext} = m_0 + h_0$; $h = |\mathbf{h}|,\ m_0 = |\mathbf{m}_0|$, and $h_0 = |\mathbf{h}_0|$. The magnetic susceptibilities are $\chi_0 = \dfrac{m_0}{h_0}$ and $\chi = \left(\dfrac{\partial m}{\partial h} \right)_{h_0, T_a}$, where $m = |\mathbf{m}|$. The variation of the magnetization of ferrofluid with its temperature is expressed in terms of the pyromagnetic coefficient $K = -\left(\dfrac{\partial m}{\partial T} \right)_{h_0, T_a}$.

It is well known that for a very slow heating of the lower boundary of the fluid layer, and in the absence of applied magnetic field, the basic temperature profile is linear and time independent and the critical condition is independent of the Prandtl number [7]. But if the fluid layer is rapidly heated from the below and cooled from the above with a large Rayleigh number, the resulting transient stability problem becomes more complex.

To proceed further, we make the system (2.1)-(2.5) dimensionless, using the thickness of the ferrofluid layer d as the characteristic distance scale, the characteristic momentum diffusion time $\dfrac{d^2}{k_T}$ as the characteristic time scale, the vertical steady temperature difference $T_1 - T_2$ as the characteristic temperature scale, and $\dfrac{K(T_1 - T_2)}{(1 + \chi)}$ as the scale for measuring magnetic field strength.

The system of equations (2.1)-(2.7) admits a basic transient state approaching a steady state for $t \to \infty$ in which the basic dimensionless temperature profiles are given by the following equations:

$$T_e = \frac{T_a}{T_1 - T_2} - z - 2\sum_{n=1}^{\infty} \frac{\sin(n\pi z)}{n\pi} \exp\{-n^2\pi^2 t\}; \tag{2.8}$$

$$T_e = \frac{T_a}{T_1 - T_2} + \sum_{n=0}^{\infty} \left[\text{erfc}\left(\frac{n}{\sqrt{t}} + \frac{z}{2\sqrt{t}}\right) - \text{erfc}\left(\frac{n}{\sqrt{t}} - \frac{z}{2\sqrt{t}}\right)\right]; \tag{2.9}$$

where the latter solution behaves well for small t and $\text{erfc}\,(z) = 1 - \frac{2}{\sqrt{\pi}} \int_0^z \exp\{-t^2\}\, dt$. In fact $T_e \to \frac{T_a}{T_1 - T_2} + \text{erfc}\left(\frac{z}{2\sqrt{t}}\right)$ for $t \to 0$. The other physical quantities in the basic state are given by,

$$\mathbf{u}_e = \mathbf{0};\ p_e = d\rho_0 g \int \{1 - \alpha(T_e(T_1 - T_2) - T_a)\} dz;\ T_a = T_1; \tag{2.10}$$

$$\mathbf{m}_e = \frac{1+\chi}{K(T_1 - T_2)} \chi_0 h_0 \hat{k} + \left(\frac{T_a}{T_1 - T_2} - T_e\right)\hat{k};\ \mathbf{h}_e = \frac{1+\chi}{K(T_1 - T_2)} h_0 \hat{k} - \left(\frac{T_a}{T_1 - T_2} - T_e\right)\hat{k}; \tag{2.11}$$

where $0 \le z \le d$ and the subscript e denotes the equilibrium state. Note that the transient decay of the basic temperature field induces the same transient character in the ferrofluid magnetic field and the ferrofluid magnetization across the ferrofluid layer. We discuss the stability of the basic transient state defined by the Eqs. (2.8)-(2.11) via investigating for the minimum critical time parameter $t = t_c$ below which the transient state prevails and above which the transient state decays.

2.1 The Stability Equations

To discuss stability of the basic state given by (2.8)-(2.11) we superimpose arbitrary perturbations on it in the form,

$$\begin{aligned} \mathbf{u} = (u, v, w);\ p = p_e + \mathscr{P}; \\ T = T_e + \theta;\ \mathbf{h} = \mathbf{h}_e + \nabla\varphi; \end{aligned} \tag{2.12}$$

where each of the perturbations, $u,\ v,\ w,\ \mathscr{P},\ \theta$, and φ are sufficiently smooth functions of the coordinates $x,\ y,\ z$, and t. In order that the system (2.12) satisfies the governing equations identically, the perturbations satisfy the following nonlinear system of partial differential equations.

$$\frac{\partial \mathbf{u}}{\partial t} + \mathbf{u}\cdot\nabla\mathbf{u} = -\nabla p_{eff} + \text{Pr}\nabla^2\mathbf{u} + \text{PrRa}\theta\hat{k} + \text{Pr}M\text{D}T(\text{D}\varphi - \theta)\hat{k} + \text{Pr}M\Phi\left(\nabla\theta + \text{D}T_e\hat{k}\right); \tag{2.13}$$

where the expression $\Phi = |\mathbf{h}| - |\mathbf{h}_e| - \text{D}\varphi$ contains second and higher order nonlinear terms in $|\mathbf{h}|$; the other equations satisfied by the disturbances are given by,

$$\frac{\partial\theta}{\partial t} + \mathbf{u}\cdot\nabla\theta = -\text{D}T_e w + \nabla^2\theta; \tag{2.14}$$

$$A\nabla^2\varphi + (1 - A)\text{D}^2\varphi - \text{D}\theta = 0; \tag{2.15}$$

$$\nabla\cdot\mathbf{u} = 0; \tag{2.16}$$

where $\mathrm{D} \equiv \dfrac{\partial}{\partial z}$, $0 \le z \le 1$; $t > 0$; z being the vertical coordinate; and p_{eff} denotes the dimensionless form of the effective fluid pressure due to hydrodynamic and thermomagnetic interactions. The dimensionless quantities which appear in Eqs. (2.13)-(2.16) are defined by,

$$\mathrm{Pr} := \frac{\nu}{k_T};\ \mathrm{Ra} := \frac{(T_1 - T_2)\alpha d^3 g}{k_T \nu};$$

$$M := \frac{\mu_0 K^2 (T_1 - T_2)^2 d^2}{\eta k_T (1+\chi)};\ A := \frac{1+\chi_0}{1+\chi}.$$

The dimensionless parameters Pr, Ra, and M are the Prandtl number, the Rayleigh number, and the thermomagnetic parameter, for the ferrofluid respectively. The dimensionless parameter $A \ge 1$ measures an extent of departure of the magnetic equation of state from its linearity. The stability of the basic state is controlled by the parameters Ra and M, each of which is a measure of the temperature difference across the ferrofluid layer. As $\mathrm{Ra} \propto (T_1 - T_2)$ and $M \propto (T_1 - T_2)^2$, it follows that Ra can take either positive or negative real values but M is always nonnegative.

The boundary conditions for the velocity field, the temperature field, and the magnetic field are given by,

$$\begin{aligned} &\text{Rigid-Boundaries:}\ \ \mathbf{u}|_{z=0,1} = 0,\ \mathrm{D}w\Big|_{z=0,1} = 0,\ \theta|_{z=0,1} = 0,\ \nabla\varphi|_{z=0,1} = 0; \\ &\text{Free-Boundaries:}\ \ \mathbf{u}|_{z=0,1} = 0,\ \mathrm{D}^2 w\Big|_{z=0,1} = 0,\ \theta|_{z=0,1} = 0,\ \nabla\varphi|_{z=0,1} = 0. \end{aligned} \tag{2.17}$$

3 The Energy Stability

Multiplying Eq. (2.13) by $\bar{\mathbf{u}}$ (where bar in $\bar{\mathbf{u}}$ denotes the complex conjugate of $\mathbf{u}$) and the Eqs. (2.14) & (2.15) by $\bar{\theta}$ and $\bar{\varphi}$ respectively; integrating the resulting equations over the system volume Ω with the utilization of the boundary conditions, divergence-free condition for $\mathbf{u}$ ((2.16)) and the divergence theorem, we obtain the following time dependent system of equations:

$$\begin{aligned} \int_\Omega \frac{1}{2\mathrm{Pr}} \frac{d}{dt} |\mathbf{u}|^2 d\Omega = &- \int_\Omega |\nabla \mathbf{u}|^2 d\Omega + \mathrm{Ra} \int_\Omega \theta \bar{w} d\Omega + M \int_\Omega \mathrm{D}T_e (\mathrm{D}\varphi - \theta) \bar{w} d\Omega \\ &+ M \int_\Omega \Phi \left(\nabla\theta \cdot \bar{\mathbf{u}} + \mathrm{D}T_e \bar{w} \right) d\Omega; \end{aligned} \tag{3.1}$$

$$\int_\Omega \frac{d}{dt} |\theta|^2 d\Omega = - \int_\Omega |\nabla\theta|^2 d\Omega - \int_\Omega \mathrm{D}T_e w \bar{\theta} d\Omega; \tag{3.2}$$

$$A \int_\Omega |\nabla\varphi|^2 d\Omega + (1-A) \int_\Omega |\mathrm{D}\varphi|^2 d\Omega = - \int_\Omega \bar{\varphi} \mathrm{D}\theta d\Omega. \tag{3.3}$$

To discuss nonlinear stability of the system, we need to investigate the time evolution of an appropriate nonnegative energy functional E which is defined as follows,

$$E(t) := \frac{1}{2\mathrm{Pr}} \|\mathbf{u}\|^2 + \lambda_1 \frac{1}{2} \|\theta\|^2 + \lambda_2 \frac{1}{2} (A \|\nabla\varphi\|^2 + (1-A) \|\mathrm{D}\varphi\|^2), \tag{3.4}$$

where $\lambda_1 > 0,\ \lambda_2 \neq 0$ are optimally chosen coupling parameters such that

$$\lambda_1 + \lambda_2 \ge 0 \ \text{ for all } \ t \ge 0;$$

$\|\cdot\|$ denotes the $\mathscr{L}^2-$norm over the Hilbert space of square Lebesgue integrable functions over the domain $\Omega \subset \mathbb{R}^2 \times [0,1]$; with the inner product $\langle f, g\rangle := \int_\Omega f\bar{g}d\Omega$.

Note that the parameter A appearing in the Eq. (3.3) satisfies $A \geq 1$ and that $\|\mathrm{D}\varphi\| \leq \|\nabla\varphi\|$; using these and the Cauchy-Schwarz inequality in the Eq. (3.3) we obtain

$$\|\nabla\varphi\|^2 \leq A\|\nabla\varphi\|^2 + (1-A)\|\mathrm{D}\varphi\|^2 = |\langle\theta, \mathrm{D}\varphi\rangle| \leq \|\theta\|\|\mathrm{D}\varphi\|$$

from which it follows that

$$\|\nabla\varphi\| \leq \|\theta\|. \tag{3.5}$$

The Eq. (3.5) along with the condition $\lambda_1 + \lambda_2 \geq 0$ justifies the nonnegativity of the energy functional i.e. $E \geq 0$.

Considering the Eqs. (3.1)-(3.3) the time rate of change of the energy functional E is given by:

$$\begin{aligned}\frac{dE}{dt} =& -\{\|\nabla\mathbf{u}\|^2 + \lambda_1\|\nabla\theta\|^2 + \lambda_2\|A\nabla^2\varphi + (1-A)\mathrm{D}^2\varphi\|^2\} \\ &+ \mathrm{Ra}\langle\theta, w\rangle + M\langle\mathrm{D}T_e(\mathrm{D}\varphi - \theta), w\rangle - \lambda_1\langle\mathrm{D}T_e w, \theta\rangle - \lambda_2\langle\mathrm{D}T_e w, \mathrm{D}\varphi\rangle \\ &+ \lambda_2\frac{(1-A)}{A}\langle\mathrm{D}\theta, \mathrm{D}^2\varphi\rangle - \lambda_2\langle\mathbf{u}\cdot\nabla\theta, \mathrm{D}\varphi\rangle + M\langle\Phi\nabla\theta, \mathbf{u}\rangle + M\langle\Phi\mathrm{D}T_e, w\rangle.\end{aligned} \tag{3.6}$$

Making transformations $\theta \to \theta/\sqrt{\mathrm{Ra}\lambda_1}; \varphi \to \varphi/\sqrt{\mathrm{Ra}\lambda_2}$, the corresponding evolution of the transformed energy functional $E \to \frac{1}{2\mathrm{Pr}}\|\mathbf{u}\|^2 + \frac{1}{2}\|\theta\|^2 + \frac{1}{2}(A\|\nabla\varphi\|^2 + (1-A)\|\mathrm{D}\varphi\|^2)$ becomes

$$\frac{dE}{dt} := \sigma E = -\mathcal{D} + R\mathcal{I} + \mathcal{N}, \tag{3.7}$$

where

$$R = \sqrt{\mathrm{Ra}}; \tag{3.8}$$

$$\mathcal{D} = \|\nabla\mathbf{u}\|^2 + \|\nabla\theta\|^2 + \|A\nabla^2\varphi + (1-A)\mathrm{D}^2\varphi\|^2; \tag{3.9}$$

$$\begin{aligned}\mathcal{I} =& \frac{1}{\sqrt{\lambda_1}}\langle\theta, w\rangle + \frac{M}{\mathrm{Ra}}\left\langle\mathrm{D}T_e\left(\frac{\mathrm{D}\varphi}{\sqrt{\lambda_2}} - \frac{1}{\sqrt{\lambda_1}}\theta\right), w\right\rangle \\ &- \left\langle\mathrm{D}T_e w, \sqrt{\lambda_1}\theta + \sqrt{\lambda_2}\mathrm{D}\varphi\right\rangle + \frac{\lambda_2}{\sqrt{\mathrm{Ra}}\sqrt{\lambda_1}}\frac{(1-A)}{A}\left\langle\mathrm{D}\theta, \frac{1}{\sqrt{\lambda_2}}\mathrm{D}^2\varphi\right\rangle;\end{aligned} \tag{3.10}$$

$$\mathcal{N} = -\frac{\lambda_2}{\sqrt{\lambda_1}}\left\langle\mathbf{u}\cdot\nabla\theta, \frac{\mathrm{D}\varphi}{\sqrt{\lambda_2}}\right\rangle + \frac{M}{\mathrm{Ra}\sqrt{\lambda_1}}\left\langle\frac{\Phi}{\sqrt{\lambda_2}}\nabla\theta, \mathbf{u}\right\rangle + \frac{M}{\sqrt{\mathrm{Ra}}}\left\langle\frac{\Phi}{\sqrt{\lambda_2}}\mathrm{D}T_e, w\right\rangle; \tag{3.11}$$

where we have made use of the easily derivable identity

$$\frac{1}{2}\frac{d}{dt}\langle A\|\nabla\varphi\|^2 + (1-A)\|\mathrm{D}\varphi\|^2\rangle = -\lambda_2\left\langle\mathrm{D}T_e w, \frac{\mathrm{D}\varphi}{\sqrt{\lambda_2}}\right\rangle - \frac{\lambda_2}{A\lambda_1}\|\mathrm{D}\theta\|^2 + \frac{\lambda_2}{\sqrt{\lambda_1}}\frac{(1-A)}{A}\left\langle\mathrm{D}\theta, \frac{1}{\sqrt{\lambda_2}}\mathrm{D}^2\varphi\right\rangle;$$

such that now

$$A\nabla^2\varphi + (1-A)\mathrm{D}^2\varphi = \frac{\sqrt{\lambda_2}}{\sqrt{\lambda_1}}\mathrm{D}\theta.$$

The scalar $\sigma = \frac{1}{E}\frac{dE}{dt}$ determines the strong nonlinear stability boundary which corresponds to

$$\sigma = 0. \tag{3.12}$$

The critical Rayleigh number at the strong energy stability limit is determined by solving the maximum problem obtained from Eq. (3.7) as the following

$$\frac{1}{R_s} = \max_{\mathcal{H}} \left(\frac{\mathcal{I}}{\mathcal{D}} \right), \tag{3.13}$$

where $\mathcal{H}$ is the underlying space of solutions. We define the basic-temporal growth rate σ_0 of the energy functional by

$$\sigma_0 = \frac{1}{E_0} \frac{dE_0}{dt};\ E_0 = \left\| T_e - \frac{T_a}{T_1 - T_2} \right\|^2. \tag{3.14}$$

The closed form expression for σ_0 is given by,

$$\sigma_0 = \begin{cases} \dfrac{1}{2t} & \text{for } \ t \leq 0.01, \\ \dfrac{24 \displaystyle\sum_{n=1}^{\infty} \exp\{-n^2\pi^2 t\} \left(1 - \exp\{-n^2\pi^2 t\}\right)}{1 - 3 \displaystyle\sum_{n=1}^{\infty} \exp\{-n^2\pi^2 t\} \left(2 - \exp\{-n^2\pi^2 t\}\right)/(n^2\pi^2)} & \text{for } \ t > 0.01. \end{cases} \tag{3.15}$$

The relaxed energy identity for the stability becomes $\sigma_0 E = R\mathcal{I} - \mathcal{D}$ which leads to the relative stability limit obtained by solving the following maximum problem,

$$\frac{1}{R_r} = \max_{\mathcal{H}} \left(\frac{\mathcal{I}}{\mathcal{D} + \sigma_0 E} \right). \tag{3.16}$$

Note that the strong-stability criterion corresponds to the relative stability criterion for $\sigma_0 = 0$.

By decomposing the solution into the standard normal modes

$$(w, \theta, \mathrm{D}\varphi) = (w(z,t), \theta(z,t), \mathrm{D}\varphi) f(x,y);\ (\nabla^2 - \mathrm{D}^2) f = -k^2 f;\ k \in \mathbb{R}$$

k being the root mean square value of the horizontal wave number, the maximum problem given by Eq. (3.16) after performing the calculus of variation, reduces to an equivalent system of Euler-Lagrange equations:

$$\begin{aligned} (D^2 - k^2)^2 w = \frac{\sigma_0}{2\mathrm{Pr}} (D^2 - k^2) w + \frac{Rk^2}{2} \left(\frac{1}{\sqrt{\lambda_1}} - \left\{ \sqrt{\lambda_1} + \frac{M}{R^2 \sqrt{\lambda_1}} \right\} \mathrm{D}T_e \right) \theta \\ + \frac{Rk^2}{2} \left(\frac{M}{R^2 \sqrt{\lambda_2}} - \sqrt{\lambda_2} \right) \mathrm{D}T_e \mathrm{D}\varphi; \end{aligned} \tag{3.17}$$

$$(D^2 - k^2)\theta = -\frac{R}{2} \left(\frac{1}{\sqrt{\lambda_1}} - \left\{ \sqrt{\lambda_1} + \frac{M}{R^2 \sqrt{\lambda_1}} \right\} \mathrm{D}T_e \right) w + \frac{\sigma_0}{2} \theta; \tag{3.18}$$

$$(D^2 - k^2)(D^2 - Ak^2)\varphi = -\frac{R}{2} \left(\frac{M}{R^2 \sqrt{\lambda_2}} - \sqrt{\lambda_2} \right) \left(\mathrm{D}^2 T_e w + \mathrm{D}T_e \mathrm{D}w \right) + \sigma_0 \frac{\sqrt{\lambda_2}}{2\sqrt{\lambda_1}} \mathrm{D}\theta; \tag{3.19}$$

along with the equation

$$(\mathrm{D}^2 - Ak^2)\varphi = \frac{\sqrt{\lambda_2}}{\sqrt{\lambda_1}} \mathrm{D}\theta, \tag{3.20}$$

and the critical stability limit is now given by the relation

$$R_r = \sup_{\lambda_1,\ \lambda_2} \inf_{k} R. \tag{3.21}$$

Observe that if we apply the operator D to the equation Eq. (3.18) and using the Eq. (3.20) in it, we obtain the differential equation similar to the one defined by the Eq. (3.19) which differ only in the coefficients independent of z. This is possible for arbitrary w if and only if the parameter λ_2 corresponds only to the extremum values of $\mathrm{D}T_e$. Consequently, we obtain λ_2 in terms of λ_1 as the following expression,

$$\lambda_2 = \frac{M\mathrm{D}T_e(z_0)}{-M\mathrm{D}T_e(z_0) + R^2}\lambda_1, \ \mathrm{D}^2T_e(z_0) = 0 \ \text{ for } \ z_0 \in (0,1). \tag{3.22}$$

Note that $\lambda_2 < 0$ but $\lambda_1 + \lambda_2 = \left(1 + \dfrac{M\mathrm{D}T_e}{-M\mathrm{D}T_e + R^2}\right)\lambda_1 = \left(\dfrac{R^2}{-M\mathrm{D}T_e + R^2}\right)\lambda_1 \geq 0$ since $-\mathrm{D}T_e \geq 0$ for all t (see also the Fig. 1 which demonstrates $-\mathrm{D}T_e \geq 0$).

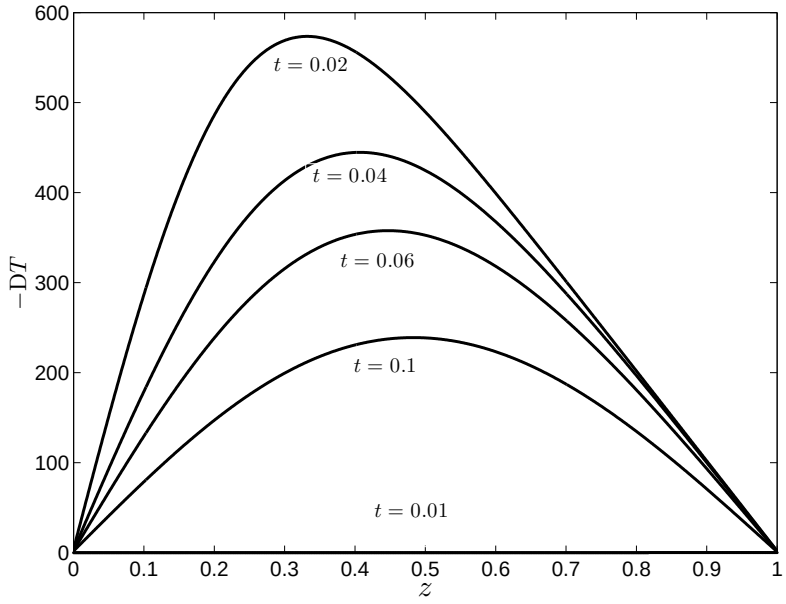

Figure 1: Variation of the derivative $-\mathrm{D}T_e$ with z for different values of t.

4 Numerical Results and Discussion

We write the equations (3.17)-(3.18) in the following equivalent matrix differential equation

$$\mathrm{D}\mathbf{Y}(z,t) = \mathbf{B}(z,t)\mathbf{Y}(z,t), \tag{4.1}$$

along with the boundary conditions

$$\begin{aligned} &\text{Rigid-Boundaries:} \ \ y_1(z,t) = y_2(z,t) = y_5(z,t) = y_8(z,t) = 0 \ \text{ for } \ z = 0,1, \\ &\text{Free-Boundaries:} \ \ y_1(z,t) = y_3(z,t) = y_5(z,t) = y_8(z,t) = 0 \ \text{ for } \ z = 0,1, \end{aligned} \tag{4.2}$$

where

$$\mathbf{Y}(z,t) = (y_1(z,t)\ y_2(z,t)\ \ldots\ y_8(z,t))';$$
$$w = y_1;\ \theta = y_5;\ \varphi = y_7;$$

$$\mathrm{D}w = y_2;\ (\mathrm{D}^2 - k^2)w = y_3;\ \mathrm{D}(\mathrm{D}^2 - k^2)w = y_4;$$
$$\mathrm{D}\theta = y_6;\ \mathrm{D}\varphi = y_8;$$

and $\mathbf{B}(z,t)$ is the underlying 8×8 coefficient matrix for the system of equations (3.17)-(3.22).

4.1 Numerical Integration

Several popular numerical schemes are available in the literature; however it appears that the stability problems are conveniently handled by the usual linear shooting method [15, 16] or a more efficient compound matrix method [3, 17, 18, 19]. If the usual linear shooting method is used, the function $\mathbf{Y}(z,t)$ is computed as a linear combination of the four linearly independent solutions $\mathbf{Y}_1(z,t),\ \mathbf{Y}_2(z,t),\ \mathbf{Y}_3(z,t),\ \mathbf{Y}_4(z,t)$ of the system (4.1)-(4.2) obtained with the following appropriate initial conditions,

$$\text{Rigid-Boundaries:} \begin{cases} \mathbf{Y}_1(0,t) = (0,0,1,0,0,0,0,0)';\ \mathbf{Y}_2(0,t) = (0,0,0,1,0,0,0,0)'; \\ \mathbf{Y}_3(0,t) = (0,0,0,0,0,1,0,0)';\ \mathbf{Y}_4(0,t) = (0,0,0,0,0,0,1,0)'; \end{cases} \tag{4.3}$$

$$\text{Free-Boundaries:} \begin{cases} \mathbf{Y}_1(0,t) = (0,1,0,0,0,0,0,0)';\ \mathbf{Y}_2(0,t) = (0,0,0,1,0,0,0,0)'; \\ \mathbf{Y}_3(0,t) = (0,0,0,0,0,1,0,0)';\ \mathbf{Y}_4(0,t) = (0,0,0,0,0,0,1,0)'; \end{cases} \tag{4.4}$$

The fact that resulting solution $\mathbf{Y}(z,t)$ should satisfy the remaining four boundary conditions at $z = 1$, leads to a secular equation of the form,

$$\det(\mathbf{\Phi})|_{z=1} = 0, \tag{4.5}$$

where we calculate for a fixed t

$$\mathbf{\Phi}_{i,j} = (\mathbf{Y}_1, \mathbf{Y}_2, \mathbf{Y}_3, \mathbf{Y}_4)_{\tau(i),j} \quad \text{for} \quad i,j = 1,2,3,4;$$

for

$$\text{Rigid boundaries:} \quad (\tau(1),\tau(2),\tau(3),\tau(4)) = (1,2,5,8).$$
$$\text{Free boundaries:} \quad (\tau(1),\tau(2),\tau(3),\tau(4)) = (1,3,5,8).$$

If the compound matrix method is used, we define in the lexicographic order $i_1 = (1,2,3,4),\ i_2 = (1,2,3,5), ..., i_{69} = (4,6,7,8),\ i_{70} = (5,6,7,8)$, and the corresponding 4×4 minors $x_{i_m},\ (m = 1,2,...70)$ of the 8×4 matrix $(\mathbf{Y}_1, \mathbf{Y}_2, \mathbf{Y}_3, \mathbf{Y}_4)$ such that the vector $\mathbf{Z} = (x_1, x_2, ..., x_{70})'$ satisfies the differential equation given by,

$$\mathrm{D}\mathbf{Z}(z,t) = \mathbf{F}(z,t)\mathbf{Z}(z,t), \tag{4.6}$$

where $\mathbf{F}(z,t)$ is a 70×70 matrix whose entries are related to the entries of the matrix $\mathbf{B}$. Elements of the matrix $\mathbf{F}$ are given by

$$\mathbf{F}_{m,n} = \begin{cases} 0 & \text{if } i_m \text{ and } i_n \text{ have at most two indices in common} \\ (-1)^{(p+q)}\mathbf{B}_{i_m(p),i_n(q)} & \text{if } i_m \text{ and } i_n \text{ differ in exactly one index} \\ \sum_{p=1}^{4} \mathbf{B}_{i_m(p),i_n(p)} & \text{if } m = n. \end{cases} \tag{4.7}$$

Here $i_m(p)$ and $i_n(q)$ stand for $p-$th and $q-$th indices in i_m and i_n, respectively.

It follows from the equation (4.4) that the initial conditions for $\mathbf{Z}$ at $z = 0$ are

$$\mathbf{Z}|_{z=0} = \begin{cases} e_{59}, & \text{for rigid boundaries} \\ e_{49}, & \text{for stressfree boundaries} \end{cases} \tag{4.8}$$

where e_{59} stands for the 70×1 column vector whose 59th entry is 1 and rest all the entries are 0. The corresponding eigenvalue relations (4.5) becomes

$$\begin{aligned} x_{12}|_{z=1} &= 0 \quad \text{for rigid boundaries} \\ x_{22}|_{z=1} &= 0 \quad \text{for free boundaries} \end{aligned} \tag{4.9}$$

The equation (4.6) with the initial condition (4.8) has been integrated in the interval $0 \leq z \leq 1$ using the Runge-Kutta Fehlberg method, to obtain $\mathbf{Z}$ and hence x_{12} and x_{22} at $z = 1$ approximately satisfying $x_{12} < 10^{-3}$ and $x_{12} < 10^{-3}$.

We have solved the system of equations (3.17)-(3.22) numerically, using the shooting method as well as the compound matrix method. The calculations involving a high Rayleigh number (R^2 of the order of 10^4) are performed using the compound matrix method while rest of the numerical calculations have been done using the shooting method.

4.2 Results for the Steady Convection

As a check for the correctness of the numerical code, we have computed numerically, the nonlinear critical Rayleigh number for the onset of the standard Rayleigh-Bénard convection in the magnetized ferrofluid layer between two horizontal rigid planes. For this we solve the set of ODE's equations (3.17)-(3.22) using the compound matrix method. The following typical values of the critical Rayleigh number and critical thermomagnetic parameter for the nonlinear stability boundary ($\sigma_0 = 0$) have been obtained:

$$R_{sc}^2(M = 0) = 1707.76, \ k_{sc} = 3.12,$$

$$M_{sc}(R_r = 0) = 3049.29, \ k_{sc} = 3.98, \ A = 1,$$

which match with the corresponding exact values of the critical Rayleigh numbers obtained for the underlying linearized problem (see Singh and Bajaj [20]). This clearly shows that for the steady ferrofluid convection problem, the critical nonlinear stability boundary coincides with the critical linear instability boundary. This rules out any possibility of subcritical instabilities in the magnetized ferrofluid layer.

4.3 The Global Stability Results

For numerical purpose we have set appropriately $n = 1000$ in Eqs. (2.8)-(2.9). When $t \to \infty$, $\sigma_0 \to 0$ and we have,

$$R_{sc} = \lim_{t \to \infty} R_{rc}. \tag{4.10}$$

For $M = 0$, we recover the global stability results for the case of ordinary fluids with consideration of different boundary conditions as shown in the Table-1. These results match with those obtained by Kim et al. [7] for ordinary fluids.

The global stability boundary of the basic transient state for the ferrofluid layer with respect to the thermomagnetic parameter, is shown in the Fig. 2 (see Table-2 for more values) for the fixed

Table 1: Variation of the critical Rayleigh number, the wave number, and the time parameter for $M = 0,\ \mathrm{Pr} = 10$, corresponding to the strong stability ($\sigma_0 = 0$.)

Boundaries	t_c	k_{rc}	R^2_{rc}	$\lim_{t\to\infty} k_{rc}$	$\lim_{t\to\infty} R^2_{rc}$
Rigid-Rigid	0.139	3.12	1699.32	3.12	1707.76
Free-Rigid	0.083	2.69	1009.95	2.68	1100.65
Free-Free	0.137	2.23	654.550	2.22	657.551

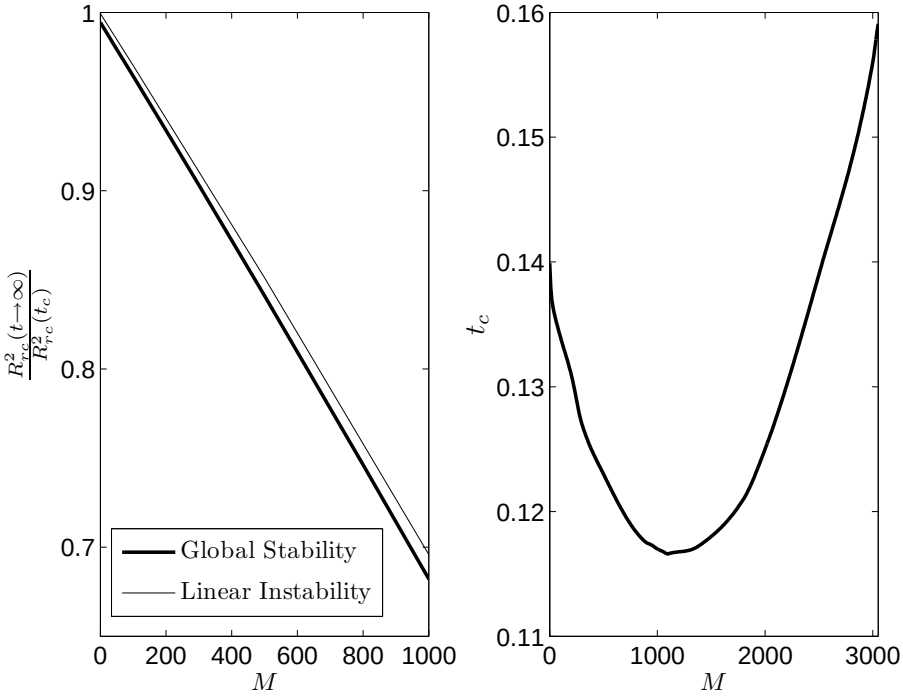

Figure 2: Comparison of the global stability results for the ferrofluid convection (Rigid-Boundaries) with the existing instability results of the Strong Stability/Linear theory for Pr = 10.

parametric values $\mathrm{Pr} = 10,$ and $\sigma_0 = 0$. The first plot in the figure gives a comparison of the critical global stability boundary with the steady strong stability boundary. The variation of the critical time t_c, as defined above with the thermomagnetic parameter, is dramatic. Initially, t_c decreases monotonically with the thermomagnetic parameter M and attains a minimum for the following values:

$$t_c = 0.11663,\ k_{rc} = 3.51,\ R^2_{rc} = 1107.009, M = 1107.009.$$

It is interesting to note that the global minimum of t_c over M occurs for $M = R^2_{rc}$. For $R^2_{rc} > M$, the critical time t_c increases monotonically with M, and this increase becomes sharp for $M > 2000$ approximately. For the gravity-free limit, the following global result has been obtained for critical value of the thermomagnetic parameter M,

$$R_r = 0,\ t_c = 0.1583;\ k_{rc} = 4.05,\ M_{rc}(\text{global}) = 3036.73.$$

For large times the corresponding values in the gravity free limit case are found to be,

$$\lim_{t\to\infty}(k_{rc},\ M_{rc}) = (3.98,\ 3049.29);$$

which match exactly with the corresponding values obtained by Finlayson [13] and Singh and Bajaj [20] using the linear instability theory. The corresponding results for the problem with

Table 2: Variation of the critical Rayleigh number (Rigid-Boundaries), the wave number, and the time parameter, with the thermomagnetic parameter M for Pr = 10, corresponding to the strong stability ($\sigma_0 = 0.$)

M	t_c	k_{rc}	$R^2_{rc}(t_c)$ (Global)	k_c	$R^2_{rc}(t \to \infty)$ (Strong-Stability)
0	0.139	3.12	1699.3	3.12	1707.7
100	0.134	3.16	1647.9	3.15	1658.1
500	0.123	3.30	1437.2	3.27	1454.4
1000	0.117	3.47	1165.9	3.43	1189.2
1500	0.118	3.64	888.87	3.58	913.20
2000	0.125	3.80	606.76	3.71	627.32
2500	0.139	3.92	318.32	3.84	332.68
3000	0.156	4.04	22.089	3.97	30.213

Table 3: Variation of the critical thermomagnetic number, the wave number, and the time parameter for $R_r = 0$ and Pr = 10, corresponding to the strong stability ($\sigma_0 = 0.$)

Boundaries	t_c	k_{rc}	M_{rc}	$\lim_{t\to\infty} k_{rc}$	$\lim_{t\to\infty} M_{rc}$
Free-Rigid	0.105	3.76	2025.002	3.57	2221.68
Free-Free	–	–	–	3.14	1558.54

free-rigid and free-free boundaries are given in the Table-3. The critical parameter t_c for the global minimum incase of free-free boundaries was not observed to occur. From Table-3, it is worthwhile to note that under the gravity free limit, the global minimum for free-rigid case is significantly lower than the one corresponding to linear instability boundary. This indicates that the transient effects are more pronounced for the case of free-rigid boundaries.

A variation of the critical onset time with the Rayleigh number for the transient convection in the ferrofluid layer is shown in the Fig. 3(a) for two typical values of the thermomagnetic parameter $M = 0$ and 10^3. The solid lines in the figure correspond to the relative stability limit while the dotted lines are drawn for the strong stability limit. It is clear from the figure that the relative stability criterion predicts a wider stability boundary than the one predicted by the strong stability criterion for $0 < t < 0.3$ approximately. Both the stability boundaries are significantly contracted with the application of magnetic field which clearly demonstrate the destabilizing action of the applied magnetic field on the base flow. A similar variation of t_c with the thermomagnetic parameter M is observed for the case of gravity free limit (Fig. 3(b)).

Unlike the conventional energy stability theory, the relative stability boundary depends upon the Prandtl number, the dependence being heavier for Pr < 1 and comparatively slighter but significant for Pr > 10. For a typical ferrofluid, the Prandtl number is always larger than unity so the Prandtl number effects can not be better demonstrated graphically. These effects are shown in the Table-4 for three different values of t and for the case of rigid boundaries. It is evident from a correlation of the data in the Table-4 that the relative stability boundary shifts towards the strong stability boundary as the Prandtl number is incremented from 10 to 100. The difference in the critical Rayleigh numbers as predicted by the two theories, is more than 100% for $t_c = 0.01$ and the difference is significant for all the three considered values of t_c in presence as well as absence of magnetic field. The tendency of applied magnetic field to advance the onset of instability is also clear from the tabulated values. In obtaining these numerical values we have

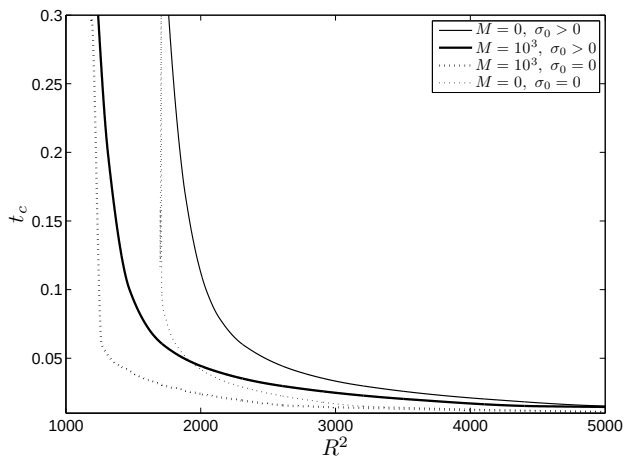

(a) The relative stability vs Strong stability

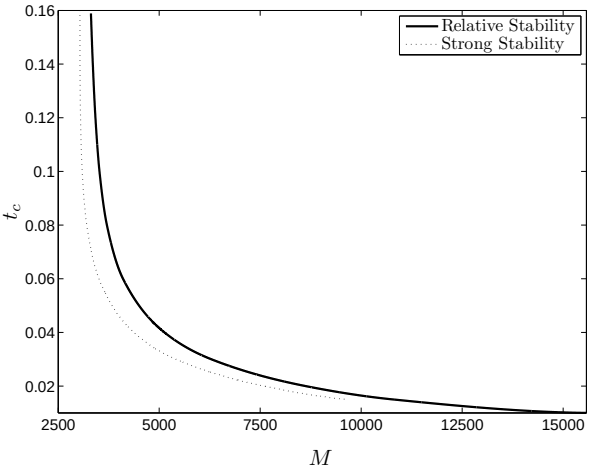

(b) The relative stability vs Strong stability

Figure 3: The relative stability vs Strong stability for the critical onset time t_c with respect to (a) R^2 for $M = 0,\ 10^3$ and (b) M for $R = 0$. The fixed parametric values are $\mathrm{Pr} = 10$ and $A = 1$.

Table 4: Variation of the critical time parameter (Rigid-Boundaries), with the Prandtl number.

Pr	M	t_c	R_r^2	R_s^2	M	R_r^2	R_s^2
10	0	0.04	2732.08	2031.10	10^3	2129.51	1483.82
		0.02	3554.76	2250.75		4146.67	2273.98
		0.01	15573.5	6831.06		15573.5	6831.06
20	0	0.04	2708.85	2031.10	10^3	2107.12	1483.82
		0.02	4095.83	2250.75		3505.80	2273.98
		0.01	15118.8	6831.06		15118.8	6831.06
10^2	0	0.04	2690.27	2031.10	10^3	2089.20	1483.82
		0.02	4055.09	2250.75		3466.55	2273.98
		0.01	14754.4	6831.06		14754.4	6831.06

observed (not shown in the Table-4) numerically that for the onset of transient convection in the ferrofluid layer, the wave number of disturbance is almost invariant under a change of Prandtl number for all t.

5 Concluding Remarks

The onset of instability in the transient Rayleigh-Bénard convection in a horizontal ferrofluid layer subjected to a vertical magnetic field, is analyzed using the energy method. A new stability criterion is derived which approaches the conventional energy stability criterion for large times. The global stability results are obtained for the underlying problem with the different boundary conditions along with incorporating the effect of the Prandtl number on the critical onset of instability. The relative stability theory reduces to the strong stability theory for the long time behavior i.e. when $t \to \infty$. This way one is able to recover the results of the conventional energy method. However for the time zone in the neighborhood of $t = 0$, the present theory predicts a more correct description of the stability boundary in a sense that now the stability limit depends upon the Prandtl number which is in accordance with the expectation of the underlying physics

of the fluid to account for the inertial effects.

It is interesting to note that with the present formulation, the steady nonlinear energy stability boundary is found to coincide with the corresponding linear instability boundary for the magnetized ferrofluid layer. Consequently, no possibility for any subcritical instabilities can arise.

The Prandtl number effects are prominent for small time scales. For the time of the order of $10^{-2} - 10^{0}$, the critical nonlinear stability boundary widens if compared with the conventional strong energy stability boundary. The wave number of disturbance for the onset of instability remains invariant with respect to the Prandtl number for all the times.

The stress-free and the rigid-free boundaries are found to be insensitive towards the time dependent stability conditions.

The present global nonlinear stability results for the onset of convection in a ferrofluid layer, impulsively heated from below, will favor the related theoretical and experimental studies in future regarding this important stability problem. Further, it would be interesting to obtain the stability equations for analyzing other time dependent basic states such as the one with temperature modulation or gravity modulation where the basic state now oscillates harmonically with respect to time with finite amplitude. The work in this direction is in progress.

5.1 Acknowledgements

A useful discussion with Dr. Parminder Singh regarding computer-programming, is gratefully acknowledged which helped the author in writing the MATLAB code for compound matrix method.

References

[1] S. Chandrasekhar. *Hydrodynamic and Hydromagnetic Stability.* Oxford University Press, Oxford, 1966.

[2] E. L. Koschmieder. *Bénard Cells and Taylor Vortices.* Cambridge University Press, Cambridge, 1993.

[3] P. G. Drazin and W. H. Reid. *Hydrodynamic Stability.* Cambridge University Press, Cambridge, 2004.

[4] E. Bodenschatz, W. Pesch, and G. Ahler. Recent developements in Rayleigh-Bénard convection. *Ann. Rev. Fluid. Mech.*, **32**:709–778, 2000.

[5] B. Straughan. *The Energy Method, Stability, and Nonlinear Convection.* Springer-Verlag, 1992.

[6] G. M. Homsy. Global stability of time-dependent flows: impulsively heated or cooled fluid layers. *J. Fluid Mech.*, **60**, 1:129–139, 1973.

[7] M. C. Kim, C. K. Choi, and D. Y. Yoon. Relaxation on the energy method for the transient Rayleigh-Bénard convection. *Physics Letters*, **A**, 372:4709–4713, 2008.

[8] Craig L. Russell, P. J. Blennerhassett, and P. J. Stiles. Weakly nonlinear stability of magnetized ferrofluids at large critical wavenumbers. *Applied Mathematics Report AMR97/17, University of New South Wales, Australia*, 1997.

[9] Craig L. Russell, P. J. Blennerhassett, and P. J. Stiles. Supercritical analysis of strongly nonlinear vortices in magnetized ferrofluids. *Proc. Roy. Soc. Lond.*, **455**, 1981:23–67, 1999.

[10] R. E. Rosenswieg. *Ferrohydrodynamics*. Cambridge University Press, Cambridge, 1985.

[11] V. G. Bashtovoy, B. M. Berkowsky, and A. N. Vislovich. *Introduction to thermomechanics of Magnetic Fluids*. Springer - Verlag, 1988.

[12] E. Blums, A. Cebers, and M. M. Maiorov. *Magnetic Fluids*. W. de Gruyter, Berlin, New York, 1997.

[13] B. A. Finlayson. Convective instability of ferromagnetic fluids. *J. Fluid Mech.*, **40**:753–767, 1970.

[14] P. J. Blennerhassett, F. Lin, and P. J. Stiles. Heat transfer through magnetized ferrofluids. *Proc. Roy. Soc. Lond.*, **433**, 1887:165–177, 1991.

[15] D. L. Harris and W. H. Reid. On the stability of viscous flow between rotating cylinders. *J. Fluid Mech.*, **20**, 1:95–101, 1964.

[16] J. Singh and R. Bajaj. Couette Flow in ferrofluids with magnetic field. *J. Magn. Magn. Mat.*, **294**:53–62, 2005.

[17] B. S. Ng and W. H. Reid. The compound matrix method for ordinary differential equations. *J. Comput. Phys.*, **58**:209–228, 1985.

[18] B. Straughan and D. W. Walker. Two very efficient methods for computing eigenvalues and eigenfunctions in porous convection problems. *J. Comput. Phys.*, **127**:128–146, 1996.

[19] V. V. Gubernov, H. S. Sidhu, and G. N. Mercer. Generalized compound matrix method. *Appl. Math. Lett.*, **19**:458–463, 2006.

[20] J. Singh and R. Bajaj. Convective instability in a ferrofluid layer with temperature modulated rigid-boundaries. *J. Fluid Mech.*, (Submitted) 2010.